Investigation of PEG embedded WO_3-graphene thin film sensor

Shivani A. Singh[1], Pravin. S. More[1*], Dattatray. J. Late[2], Rajesh W. Raut[3]

[1]*Department of Physics, Institute of Science, Madam Kama Road, Fort Mumbai-400032, India*
[2]*Physical and Materials Chemistry Division, CSIR-National Chemical Laboratory, Pune - 411 008, India*
[3]*Department of Botany, Institute of Science, Madam Kama Road, Fort Mumbai-400032, India*

[*]Corresponding author: Tel.: (+91) 9403983544; (+91) 8983537330; E-mail:psmore.ism@gmail.com, p_smore@yahoo.co.in

Received: 28 May 2016, Revised: 29 September 2016 and Accepted: 16 June 2017

DOI: 10.5185/amp.2017/807
www.vbripress.com/amp

Abstract

In the present investigation, we demonstrated the fabrication of polyethylene glycol (PEG) embedded a WO_3-graphene film. Transparent and electrically composite films of polyethylene glycol (PEG) were fabricated on ITO coated substrate by incorporation of WO_3-graphene Nano sheets into PEG followed by spin coating and chemical reduction. The obtained film exhibited good sensitivity for H_2 and LPG gas sensing applications to be used in diverse areas.

Keywords: Polyethylene glycol, graphene, WO_3, sensor, thin film.

Introduction

The graphene is a miracle material that appeals countless interests in material science and condensed matter physics. It is the liveliest and also the sturdiest material ever measured **[1-3]**. The unique band structure displayed by it in combination with the physical properties its harbour find tremendous application prospects. With large surface-to-volume ratio, sole optical properties; exceptional electrical conductivity, great carrier mobility and density, high thermal conductivity graphene becomes one of the best suited candidate for sensor applications. The property displayed by the graphene has ability to detect even single molecule of toxic gas. The large surface area provides a platform for loading of preferred biomolecules, and exceptional conductivity and lesser band gap can be beneficial for conducting electrons between biomolecules and the electrode surface. Graphene based sensors can be miniaturize and being lighter in weight might provide endless design possibilities. Graphene based sensors are sensitive and able to detect even smaller changes in signal, expected to be faster and eventually less expensive than traditional sensors. Some graphene-based sensor designs contain a Field Effect Transistor (FET) with a graphene channel **[4]**. Transparent electrodes have been widely used in electronic devices such as solar cells, displays, and touch screens. Highly flexible transparent electrodes are especially desired for the development of next generation flexible electronic devices. Although indium tin oxide (ITO) is the most commonly used material for the fabrication of transparent electrodes, its brittleness and growing cost limit its utility for flexible electronic devices.

Upon binding of an analyte to the prototype sensor, the current through the transistor changes, the change in the current can be sense as a signal, that can be analysed and determine at several variables **[5]**. Graphene-based Nano electronic devices have also been researched for their use in different applications **[6]**. Graphene also exhibit change in the conductance as a function of extent of surface adsorption, large specific area and low Junction noise, because of these properties graphene becomes a promising candidate to detect a variety of toxic and pollutant gas molecules. In combination with the polymer nano composites, Graphene emerges as one of the most scientifically advanced material from the traditional graphene-based materials and polymer materials.

Experimental

Materials/ chemicals details

In the present study, the commercially available polyethylene glycols (PEG-8000 LR) and indium tin oxide (ITO) [S.D. Fine Chem. Ltd.] were used. The graphene flakes were synthesized using modified Hammers method (REF).

Material synthesis / reactions

For preparation of PEG embedded WO_3-graphene, thin film of graphene was coated on ITO substrate. Then, 10gm of the PEG-8000 LR (Polyethylene glycol) was thoroughly mixed with 10 ml of water. The indium tin oxide (ITO) substrate were cleaned with acetone, ethanol and then deionized water for 10 min successively, under the assistance of ultra-sonication. On ITO substrate, a

single groove of 0.5mm of depth was made on which the paste of WO_3-Graphene modified with PEG as a sensing material was coated. The PEG embedded WO_3-Graphene thin film was obtained after drying at room temperature for 24 hrs.

Material's characterizations

For the identification of crystal phase and to calculate various structural parameters of the obtained sample, X-ray diffraction (XRD) pattern were recorded using XPERT-PROMPD X-ray diffractometer, with CuKα radiation (λ = 1.5405 Å) in 2θ range of 10-80. The Raman spectroscopy was recorded with a (LabRAM HR) using Ar laser (514.5 nm) in the back-scattering geometry. The Surface morphology of the synthesized products was observed using scanning electron microscopy (SEM) (JEOL, JSM-IT300) and the particle analysis of PEG embedded Graphene sample was carried out by Nano particle tracking analysis (NTA) Version 2.3 Build 0033 LM-20, Nano sight UK.

Results and discussion

For the Raman spectra of graphene, the sample was dispersed in ethanol and drop was casted onto the substrate. The Raman spectrum was recorded after the evaporation of the solvent at room temperature, with a (LabRAM HR) using Ar laser (514.5 nm) in the back-scattering geometry. The laser power used on the sample was ~0.5 mW for 514.5 nm to avoid possible heating effect by the laser. The size of the laser spot was ~ 1 μm. The typical Raman spectra of graphene sheet shows D band ~ 1350 cm^{-1} and G band ~ 1600 cm^{-1} and a small intense 2D band ~ 2800 cm^{-1} as depicted in **Fig. 1.**

The morphological studies were carried out by using scanning electron microscope (SEM). It can be seen from the figure that most of PEG-WO_3-graphene nanosheet sample surface shows random orientation of sheet embedded on substrate as shown in **Fig. 2(a-b).**

The particle analysis of PEG embedded Graphene sample was carried out by nanoparticle tracking analysis (NTA) Version 2.3 Build 0033 Nano sight. The small pieces of graphene sample were ultrasonicated 20 mins with 500 watt. The **Fig. 3(a-b)** shows the Brownian motion of Nano particles in snap shot and **Fig. 3 (c-d)** shows the particle size vs relative intensity plot respectively. The drift velocity of WO_3-Graphene embedded PEG sample is found to be ~ 4424 nm/s.

Fig. 4 shows the typical sensor device based on WO_3-graphene embedded PEG sample. The sensitivity factor was monitored for H_2 and LPG gases as a function of temperature. The highest sensitivity factor for both the gases was found to be at a lowest optimum operating temperature of ~ 53^0C. In case of LPG the highest sensitivity factor was observed to be ~ 2x 1011, whereas for H_2 it is ~ 4.7x1011. The large difference in sensitivity factor indicates the high sensitivity of WO_3-graphene sheet embedded PEG sample towards H_2.

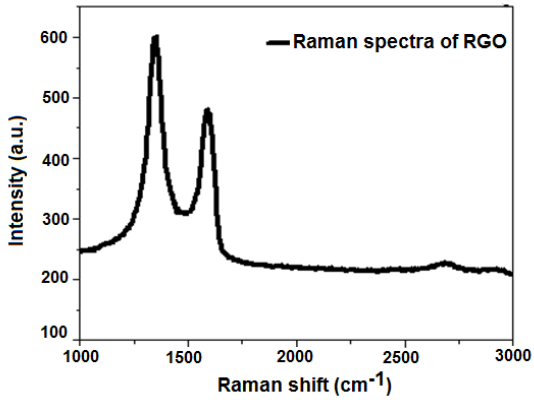

Fig. 1. Raman spectra of pristine RGO sample.

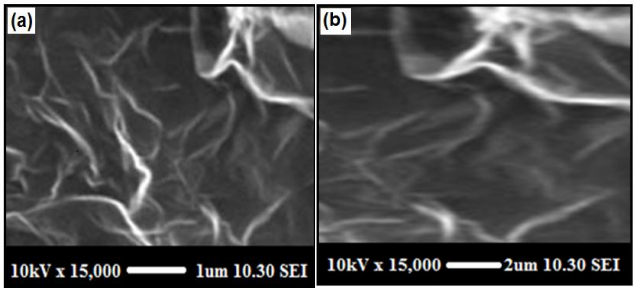

Fig. 2. (a) and (b) SEM images of WO_3-Graphene embedded PEG sample.

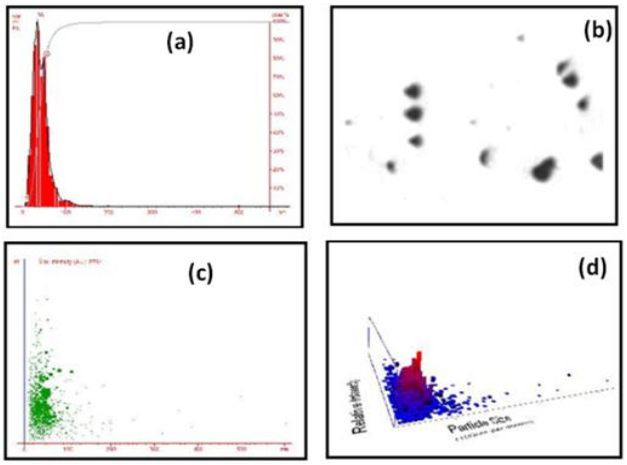

Fig. 3. Nanoparticle Tracking Analysis (NTA) report (a) Particle Size / Concentration (b) Sample Videosnap shot (c) Particle Size / Relative Intensity (d) Particle Size / Relative Intensity 3D plot.

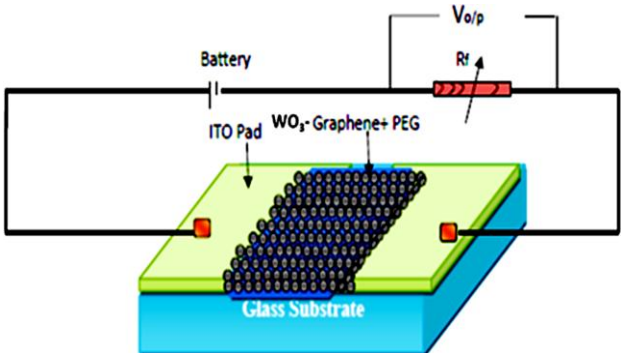

Fig. 4. Typical gas sensor device of PEG embedded WO_3-graphene fabricated on ITO substrate.

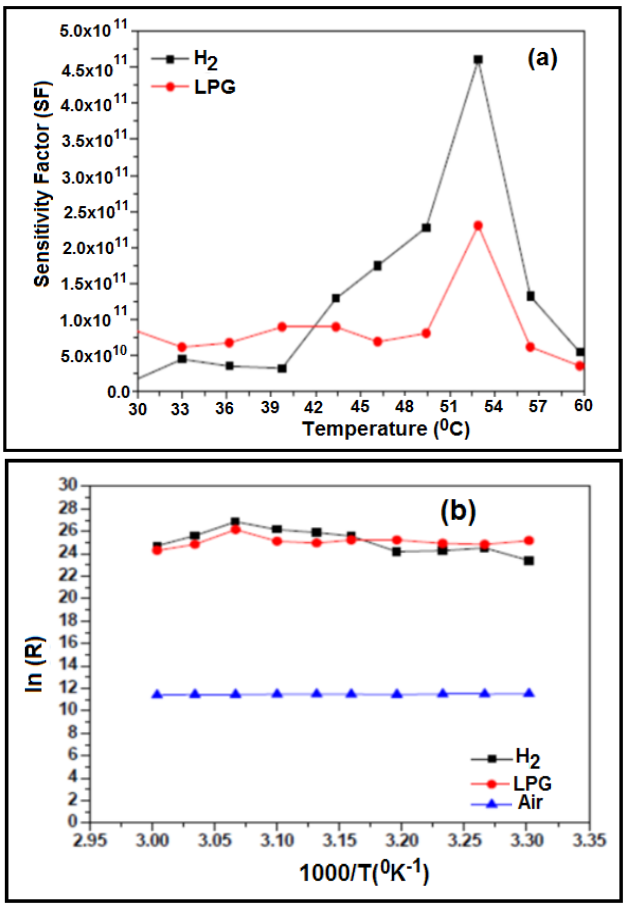

Fig. 5 (a) Variation of sensitivity with respective temperature for H_2 and LPG gases (1000 PPM), (b) Arrhenius plot for PEG embedded WO_3-graphene sample.

The response of the sensing material towards gas with increase in the temperature has been investigated. The typical response time and recovery time were found to be ~ 1 sec. Temperature is an important variable to measure sensitivity. **Fig. 5** shows the relative resistance of the sample which increases linearly with increase in the temperature up to an optimum operating temperature and later decreases over a range. The response of sensor toward gas can be given in terms of relative variation, ΔR i.e. (R_g-R_a), of the sensor resistance at a given temperature, where R_a is the initial resistance of the sensor and R_g is the resistance for different gases. **Fig. 5** shows the changes in ΔR against temperature. The sensitivity of sample was determined from the slope of ΔR with respective R_a.

The activation energy (ΔE) is the measure of the thermal or other form of energy that is required to raise the electrons from the donor levels to the conduction band or to receive electrons by the acceptor levels E_a from the valence band. The measurement of the activation energy by thermal resistance method can be calculated from the variation of σ or ρ and expediently R with the temperature, it is observed that the activation energy in case for H_2 at an optimum operating temperature of ~ 53^0C is ~2.4 eV and for LPG it is ~2.5 eV. It is evident that slight change in the temperature will alter the resistance because the coverage as well as chare of the surface species (O_2, $2O^-$, O^- or O^{2-}) can be altered in this process. The deviation from the straight-line behavior can be attributed to the large and small particle sizes of materials. In the overall conduction process a contribution arising from the participation of PEG embedded WO_3 graphene of lower average nanosheet thickness and with larger surface area i.e., the distribution of thickness, dominates in thermally activated conduction process **[7-12]**. Following simplified expressions $\rho = \rho_0 e^{(-\Delta E/2KT)}$, can be used to calculate the temperature dependence of resistivity for a semiconducting material, this can be further simplified to $\ln R = R_o e^{(-\Delta E/2KT)}$ for resistance, since dimensions remain unchanged during small temperature variations. The activation energy of PEG embedded WO_3 graphene materials was calculated as per the following equations, activation energy, $\Delta E = (E_c-E_v) / 2 = E_g$, Here, Ec and E_v are energy values corresponding to bottom-edge of the conduction band and the top edge of the valence band respectively, E_g is the band gap of the semiconductor, T is the absolute temperature of the material and K is the Boltzmann constant. The temperature resistance plot in the form of ln R and (1/T), known as Arrhenius plot, has a slope of ($\Delta E/2K$) according to equation $\ln R = R_o e^{(-\Delta E/2KT)}$ measuring the slope of Arrhenius plot of a linear zone **[13-16].**

Conclusion

The Present study reports the preparation of WO_3-graphene embedded PEG sample. A simple mechanical technique for low-density polyethylene film coated by multilayer graphene has been described. The favorable interactions between PEG and WO_3-Graphene were confirmed by Raman spectroscopy, SEM and particle analysis. The temperature dependence of the electrical resistance of PEG embedded WO_3-Graphene sample was investigated. The experimental results leads to a nano composite film sensor with high sensitivity ($SF = 4.5X10^{11}$) with low activation energy of 2.4 eV for H_2 and low sensitivity for LPG ($\sim 2.0X10^{11}$) with an activation energy of 2.5eV. The advantage of this approach is cheap and simple fabrication procedure. The obtained film exhibited good sensitivity for H_2 gas sensing applications in diverse areas.

Acknowledgements

One of the authors P. S. More is thankful to University Grant Commission (UGC), New Delhi, India for financial support.

References

1. K. S. Novoselov; A. K. Geim; S. V Morozov; D. Jiang; Y. Zhang; S. V Dubonos; I. V Grigoriev; A. A. Firsov; *Science (New York, N.Y.)*, **2004**, 306,666.
DOI: 10.1126/science.1102896
2. L. Brown; R. Hovden; P. Huang; M. Wojcik; D. a. Muller; J. Park; *Nano Letters*, **2012**, 12, 1609.
DOI: 10.1021/nl204547v

3. H. P. Boehm; A. Clauss; G. Fischer; U. Hofmann; *Fifth Conference on Carbon*, **1962**, 73. **DOI:** 10.1016/B978-0-08-009707-7.50013-3
4. R. H. Bari; S.B. Patil; A. R. Bari; *International Journal on Smart Sensing and intelligent systems*, **2014**, 7, 610. **DOI:** 10.1007/s12034-011-0045-0.
5. G. Eda; G. Fanchini; M. Chhowalla; *Nature nanotechnology*, **2008**, 3, 270. **DOI:** 10.1038/nnano.2008.83
6. Y. Wang; X. Chen; Y. Zhong; F. Zhu; K. P. Loh, *Applied Physics Letters*, **2009**, 95, 123. **DOI:** 10.1063/1.3204698
7. S. Kochmann; T. Hirsch; O. S. Wolfbeis; *TrAC - Trends in Analytical Chemistry*, **2012**, 39, 87. **DOI:** 10.1016/j.trac.2012.06.004
8. L. David; R. Bhandavat; G. Kulkarni; S. Pahwa; Z. Zhong; G. Singh; *ACS Applied Materials and Interfaces*, **2013**, 5, 546. **DOI:** 10.1021/am301782h
9. C. S. Boland; U. Khan; C. Backes; A. O'Neill; J. McCauley; S. Duane; R. Shanker; Y. Liu; I. Jurewicz; A. B. Dalton; J. N. Coleman; *ACS nano*, **2014**, 8, 8819. **DOI:** 10.1021/nn503454h
10. P. G. Collins; K. Bradley; M. Ishigami; A. Zettl; *Science*, **2000**, 287,1801. **DOI:** 10.1126/science.287.5459.1801
11. S. Zeng; D. Baillargeat; H.-P. Ho; K.-T. Yong; *Chemical Society reviews*, **2014**, 43, 3426. **DOI:** 10.1039/c3cs60479a
12. M. Iqbal; M. A. Gleeson; B. Spaugh; F. Tybor; W. G. Gunn; M. Hochberg; T. Baehr-Jones; R. C. Bailey; L. C. Gunn; *IEEE Journal on Selected Topics in Quantum Electronics*, **2010**, 16, 654. **DOI:** 10.1109/JSTQE.2009.2032510
13. T. Anderson; F. Ren; S. Pearton; B. S. Kang; H.-T. Wang; C.-Y. Chang; J. Lin; *Sensors (Basel, Switzerland)*, **2009**, 9, 4669. **DOI:** 10.3390/s90604669
14. B. Mailly-Giacchetti; A. Hsu; H. Wang; V. Vinciguerra; F. Pappalardo; L. Occhipinti; E. Guidetti; S. Coffa; J. Kong; T. Palacios; *Journal of Applied Physics*, **2013**, 114, 484. **DOI:** 10.1063/1.4819219
15. D. Grieshaber; R. MacKenzie; J. Vörös; E. Reimhult; *Sensors*, **2008**, 8, 1400. **DOI:** 10.3390/s8031400
16. Q. Liang; X. Yao; W. Wang; Y. Liu; C. P. Wong; *ACS Nano*, **2011**, 5, 2392. **DOI:** 10.1021/nn200181e

